MASS Transfer of a Solubilizate in a Micellar Solution and Across an Interface

Christie L. Williams,† Ashok R. Bhakta,‡ and P. Neogi*

Chemical Engineering Department, University of Missouri—Rolla, Rolla, Missouri 65409-1230

Received: November 17, 1998; In Final Form: February 22, 1999

A water insoluble material, when it is to be moved through a water phase to be delivered into an oil phase, can be conveniently solubilized in a detergent micelle. In that form, it can exist in water at higher concentrations and pass easily into the oil phase for which it has a higher affinity. We have measured the mass transfer rates in water as well as those across the interface. The mass transfer rates in such systems are very low which make them difficult to measure. An experimental setup which is capable of making these measurements is presented. A spatio-temporal variation of concentration is induced inside a spectrophotometer cuvette. As the system moves toward equilibrium under diffusion, the change in concentration with time is monitored by measuring the absorbance of the solution. The solution to the appropriate boundary value problem is used to back calculate the diffusivity and interfacial resistance from the absorbance data using the fact that absorbance is linearly dependent on concentration. Satisfactory values of diffusivities are reported for simple solutes and a surfactant, sodium dodecyl sulfate, SDS (the last has been reported earlier, Neogi,1994) in water. This technique has been used to measure the transport of nitrobenzene from SDS micelles to squalane. The results indicate significant interfacial resistance. A quantitative model has been provided for the first time.

Introduction

Much of the work involving mass transfer in surfactant systems has been conducted in concentrated solutions.[1,8,9,18,19,22,23,27,29,30−32] Diffusion in the bulk phases is seen to be important, although investigators differ in their opinion on the importance of interfacial resistance to mass transfer. This resistance is associated with the breakdown of a surfactant microstructure and the formation of another at the interface. Existence of such a resistance has been demonstrated in micellar solutions, which are surfactant solutions of lower concentrations, during the process of solubilization of a solid oil.[4,34] Very clear indications of interfacial resistance as the dominant mechanism in the solubilization of oils have been reported by Carroll[3] and Chen et al.,[5] where the last reference is from a group that in their work over a decade in similar experiments, had encountered, according to them, only the diffusional resistances.[19,29−32] The possiblity of interfacial resistance as the controlling resistance has been also raised by Kabalov.[13] The conclusion that during the solubilization of a solid there exists a significant resistance at the solid surface was also reached by Grimberg et al.[10] Generally, only numerical values for the interfacial resistances could be obtained, and only in some cases. That is, there is no quantitative model.

The problem of interest here is that of drug delivery through with a micellar solution. Here a water insoluble drug is solubilized in a micellar solution (and in instances involving vesicles and liposomes).[16] When the drug reaches the target, such as a nerve in the case of anesthetics, it demicellizes on that surface to give off the solubilized material inside to the nerve. The nerve can be taken to be a water insoluble material or "oil," in which the anesthetic dissolves. The outside resistance due to diffusion of the micelles containing the solubilizate to the interface and the interfacial resistance when the micelle breaks down to give up the drug to the nerve/oil are the two resistances to mass transfer that are encountered. These have been shown schematically in Figure 1. It is noteworthy that detergency works in the reverse sequence.

Weinheimer, Cussler, and Evans[36] have measured the diffusivity of the surfactant in a micellar solution as a whole, without distinguishing the diffusivity of singly dispersed amphiphiles from that of a micelle, using a very successful model. One case was considered in which a hydrophobic dye was solubilized in a micellar solution and the dye diffusivity was measured. It constituted the first study of the transport of a solubilizate. However, data interpretation for such a system becomes very difficult because both surfactant and the solubilizate are diffusing simultaneously. The measurements were made using Taylor's dispersion.

Armstrong et al.[2] have made measurements of the transport of solubilizates of varying degrees of hydrophobicity using Taylor's dispersion. Their results were interpreted using a simple but ad hoc model which frequently led to unsatisfactory answers.

Hadkar and Angane[11] have measured the rates of diffusion of drugs across a porous glass membrane and it was found that the transport increased significantly in the presence of a micellar solution.

There does not seem to be any clear study of the diffusivity of a solubilizate in a micellar solution. There are many measurements of NMR self-diffusion coefficients,[21] but these are difficult to interpret. Furthermore, there are no studies on the interfacial resistance of transfer of a solubilizate in liquid−liquid systems, a feature that interests us the most.

In the experiments described below, we have discarded the use of convection, which slows down our experiments considerably, but have placed our system in a more protected environment of a spectrophotometer cuvette following Maramatsu and Minton.[24] They introduced a known amount of protein solution in a spectrophotometer cuvette. Next, they added a solution at a different concentration on top of the lower solution, leading

† Present address: Covance Research Triangle, North Carolina.
‡ Present address: Aspen Technology, Inc., Cambridge, Massachusetts.

10.1021/jp984448m CCC: $18.00
Published on Web 04/07/1999

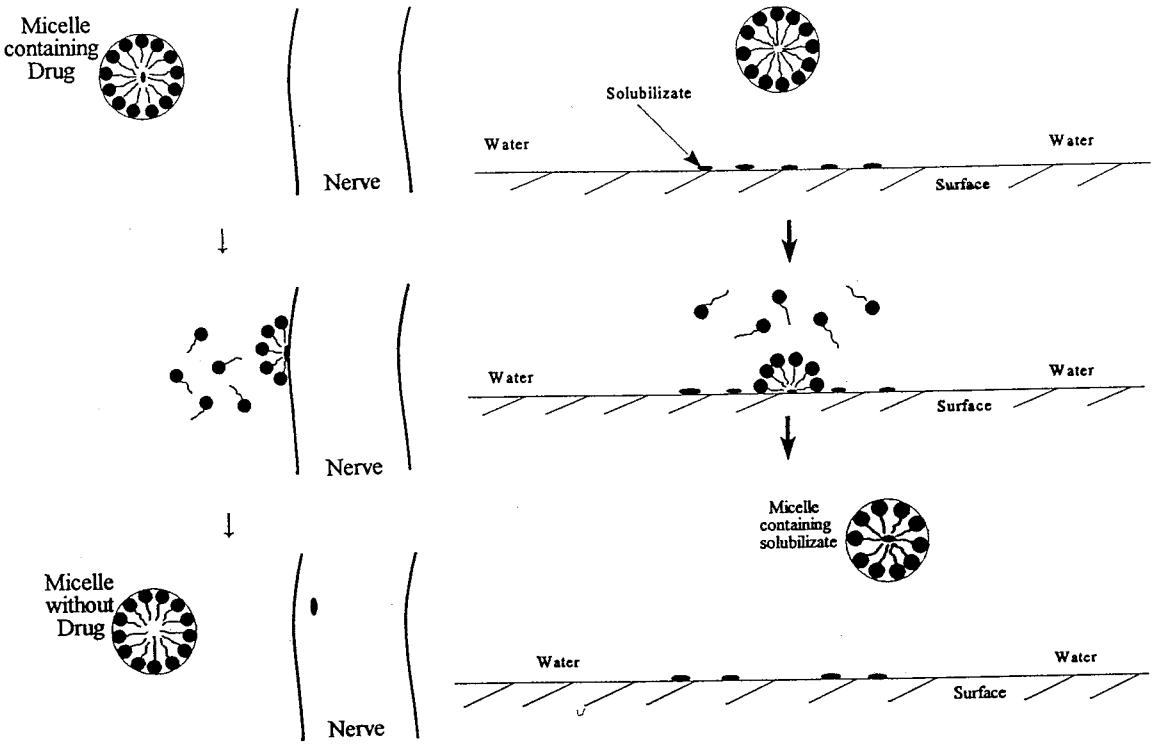

Figure 1. Schematic diagram of how a solubilizate is transferred from a micellar solution into an oil phase. The surfactant is insoluble in oil.

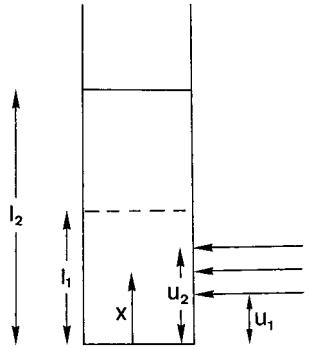

Figure 2. The various lengths involved are shown on the cuvette. The dimensions u_1 and u_2 are fixed, and u_2 is always less than l_1.

to a sharp initial concentration gradient inside the spectrophotometer cuvette. As diffusion proceeded, changes in concentrations were monitored by absorbance measurements. The measured profiles were fitted to the theoretical curves to compute the values of the diffusivities. It is very important in this experiment to get a flat initial interface. They designed an elaborate delivery system which, according to them, eliminated any impact while layering one fluid on top of another. This technique eliminated the usual six-valve stopped-flow system used to get sharp interfaces in interferometric measurements. They also designed a mechanized system for tracking the interface. This allowed them to measure a profile (actually a very sharply changing one) quickly and hence calculate the diffusivities quickly. That is, the fast tracking system eliminates the long wait for the profiles to change appreciably. In some sense, the attachments make the method somewhat like a simplified synthetic boundary experiment.

We simplified the setup and eliminated the moving part which is neither easy to fabricate nor easy to operate. A brief description of the technique and setup (see Figure 2) is given below. A known volume of the first liquid was introduced into the spectrophotometer using a micropipet. Since the cross-sectional area is known, the height l_1 can be calculated accurately. The second fluid was layered on top of the first using a Rame-Hart micrometer syringe. The tip of the needle was placed very close to the wall and very near the liquid surface. When the barrel was rotated to deliver the liquid, the tip of the needle would also rise, thus always remaining very close to the surface. Typically, it took about 5 min to deliver the top liquid. Because the volume delivered was known, the total height l_2 could be calculated. The lower portion of the cuvette was partially blacked out using tape, leaving exposed a smaller opening for the beam, from u_1 to u_2. That made the beam width exactly known. The dimensions are illustrated in Figure 2.

The boundary value problem becomes

$$\frac{\partial c}{\partial t} = D\frac{\partial^2 c}{\partial x^2} \tag{1}$$

with

$$c = c_{1o} \qquad \text{from } x = 0 \text{ to } l_1$$

$$c_{2o} \qquad \text{from } x = l_1 \text{ to } l_2 \text{ at time } t = 0$$

and

$$\frac{\partial c}{\partial x} = 0 \text{ at } x = 0 \text{ and } x = l_2$$

This is solved easily using Laplace transforms. We are interested in the quantity

$$\langle c \rangle = \frac{1}{u_2 - u_1}\int_{u_1}^{u_2} c\, dx \tag{2}$$

which is the average concentration as seen by the spectrophotometer. The solution to eq 1 is given by

$$\theta = \frac{c_{1o} - c_{2o}}{c_{1o} - c_\infty}\frac{l_2}{u_2 - u_1}\sum_{n=1}^{\infty} B_n \frac{(-1)^n}{n^2\pi^2}\left[1 - \exp\left(-\frac{n^2\pi^2 Dt}{l_2^2}\right)\right] \quad (3)$$

where c_∞ is the concentration at infinite time and

$$\theta = \frac{c_{1o} - \langle c\rangle}{c_{1o} - c_\infty}$$

and

$$B_n = \cos\left(n\pi\frac{u_2 + l_2 - l_1}{l_2}\right) - \cos\left(n\pi\frac{u_2 - l_2 + l_1}{l_2}\right) - \cos\left(n\pi\frac{u_1 - l_2 + l_1}{l_2}\right) + \cos\left(n\pi\frac{u_1 - l_2 + l_1}{l_2}\right)$$

Note that θ is zero at $t = 0$, and 1.0 at infinite time. The solution at short times (holds up to 50% completion) is simpler and is given by

$$\theta = \frac{c_{1o} - c_{2o}}{c_{1o} - c_\infty}\frac{\sqrt{D}}{\sqrt{\pi}(u_2 - u_1)} \times \left[\sqrt{t}\left(\exp\left(-\frac{(l_2 - u_2)^2}{4Dt}\right) - \exp\left(-\frac{(l_1 - u_1)^2}{4Dt}\right)\right) - \frac{\sqrt{\pi}}{2}\left(\frac{l_1 - u_2}{\sqrt{D}}\,erfc\left(\frac{l_1 - u_2}{2\sqrt{Dt}}\right) - \frac{l_1 - u_1}{\sqrt{D}}\mathrm{erfc}\left(\frac{l_1 - u_1}{2\sqrt{Dt}}\right)\right)\right] \quad (4)$$

Now, if Beer's law holds, the absorbance A is proportional to concentration, and

$$\frac{c_{1o} - c_{2o}}{c_{1o} - c_\infty} = \frac{A_{1o} - A_{2o}}{A_{1o} - A_\infty} \qquad \text{and} \qquad \theta = \frac{A_{1o} - \langle A\rangle}{A_{1o} - A_\infty}$$

For the conditions of our experiments, since the upper liquid is initially free of solute, $A_{2o} = 0$, and $A_\infty = A_{1o}\, l_1/l_2$. It is evident that if Beer's law is not observed, a numerical procedure will be required to get absorbance as a function of concentration.

When the top and bottom fluids are different and immiscible (oil and micellar solution) the theory is more difficult. If c_1 ($0 \le x < l_1$) and c_2 ($l_1 < x \le l_2 - l_1$) are the concentrations of the solubilizate in the bottom and the top phases, then the conservation equations are

$$\frac{\partial c_1}{\partial t} = D_1\frac{\partial^2 c_1}{\partial x^2} \quad (5)$$

$$\frac{\partial c_2}{\partial t} = D_2\frac{\partial^2 c_2}{\partial x^2} \quad (6)$$

The boundary conditions of impermeability are

$$\frac{\partial c_1}{\partial x} = 0 \qquad \text{at} \qquad x = 0$$

$$\frac{\partial c_2}{\partial x} = 0 \qquad \text{at} \qquad x = l_2$$

Since the solute is initially present in the lower phase only, the initial conditions are $c_1 = c_{1o}$ and $c_2 = 0$. The surfactant does not dissolve in oil. The condition of transfer of the solubilizate at the liquid−liquid interface is

$$-D_1\frac{\partial c_1}{\partial x} = k_i(c_1 - Kc_2) = -D_2\frac{\partial c_2}{\partial x} \qquad \text{at} \qquad x = l_1 \quad (7)$$

Equation 7 contains the model for interfacial resistance, in that the local equilibrium is assumed to not hold there and k_i is the interfacial conductance. If k_i is infinite, local equilibrium and zero interfacial resistance of a classical system returns. K is the partition coefficient, which is the concentration in the micellar solution divided by the concentration in the oil phase. The solution in the Laplace domain is

$$\overline{\langle c_1\rangle} = \frac{\left[\sinh\left(u_2\sqrt{\left(\frac{s}{D_1}\right)}\right) - \sinh\left(u_1\sqrt{\left(\frac{s}{D_1}\right)}\right)\right]k_i c_{1o}\sqrt{D_2}N}{s\sqrt{\left(\frac{s}{D_1}\right)}(u_2 - u_1)M} + \frac{c_{1o}}{s} \quad (8)$$

where

$$N = \cosh\left(l_1\sqrt{\left(\frac{s}{D_2}\right)}\right)\sinh\left(l_2\sqrt{\left(\frac{s}{D_2}\right)}\right) - \cosh\left(l_2\sqrt{\left(\frac{s}{D_2}\right)}\right)\sinh\left(l_1\sqrt{\left(\frac{s}{D_2}\right)}\right)$$

and

$$M = \left[-\sqrt{(sD_1D_2)}\sinh\left(l_1\sqrt{\left(\frac{s}{D_1}\right)}\right) - k_i\sqrt{(D_2)}\cosh\left(l_1\sqrt{\left(\frac{s}{D_1}\right)}\right)\right] \times \left[\cosh\left(l_1\sqrt{\left(\frac{s}{D_2}\right)}\right) - \cosh\left(l_2\sqrt{\left(\frac{s}{D_2}\right)}\right)\sinh\left(l_1\sqrt{\left(\frac{s}{D_2}\right)}\right)\right] + \sqrt{D_1}k_i\mathrm{K}\sinh\left(l_1\sqrt{\left(\frac{s}{D_1}\right)}\right)\left[\sinh\left(l_1\sqrt{\left(\frac{s}{D_2}\right)}\right) \times \sinh\left(l_2\sqrt{\left(\frac{s}{D_2}\right)}\right) - \cosh\left(l_2\sqrt{\left(\frac{s}{D_2}\right)}\right)\cosh\left(l_1\sqrt{\left(\frac{s}{D_2}\right)}\right)\right]$$

It is impossible to invert the equation for subsequent parameter estimation. The Heaviside inversion formula requires that we have to find eventually the roots of an equation. However, this equation contains the unknown parameters. It is also sufficiently complicated that the roots can only be found numerically even if the parameters were specified. Hence this approach, which is useful in the problem where the two solvents are both water, fails here. The method of moments gave impossibly long expressions (*Mathematica* output was more than 200 pages), and was abandoned. However, parameter estimation can be done in the Laplace domain.[12,17] Since we know that Heaviside inversion should work in a diffusion problem, that is, the solution is a series of exponentials, we can fit the experimental data to a set of exponentials and then take a Laplace transform of this series and find a set of parameters D_1, D_2, k_i, and K, which would make this equation in the Laplace domain fit eq 8 at sufficient number of points of real values of s, the Laplace variable.

We emphasize here that the present geometry allows one to provide the full details of the mechanisms of transport in the two phases, as well as at the interface. This is not possible in the systems studied by Carroll,[3] Chen et al.,[5] or Kabalnov.[12]

TABLE 1: Estimated Parameters for Nitrobenzene (NB) Transport

	concd SDS (mM)	concd NB (mM)	$D_1 \times 10^8$ (m^2/s)	$D_2 \times 10^{10}$ (m^2/s)	$K \times 10^2$	$k_i \times 10^4$ (cm/s)
1	30	0.027	5.65	6.49	9.04	5.82
2[a]	30	0.048	5.65	6.73	8.53	5.76
3	30	0.097	5.73	7.56	7.98	5.64
4[a]	60	0.097	5.68	7.87	8.48	0.35
averages			5.68 (±0.5%)	7.16 (±10%)	8.51 (±6%)	5.74 (±1.7%, 4, excluded)

[a] 2 and 4 share the same SDS to NB ratio.

Experimental Section

Two sets of experiments were performed. In the first set an aqueous solution was the lower phase and pure water was the top phase.

Distilled water was used. Reagent grade KNO_3, aniline, phenol, and nitrobenzene were the components used in the lower aqueous solution. Sodium dodecyl sulfate (SDS) was twice recrystallized from ethanol. A Hitachi U-2000 double beam spectrophotometer with a "reconstructed" thermostated cell chamber, was the instrument used to measure the changes in the absorbance. All experiments were carried out at 30 °C. Most solutions were 1 wt %, except for SDS. Some were at much lower concentrations. For each solute, an absorbance-concentration curve was first established to verify that Beer's linear law applied for every species. A predetermined volume of solution of known concentration was poured into a quartz cuvette using Eppendorf micropipets (readability of up to 1 μL). The absorbance (A_{1o}) was read and the volume introduced was noted. Pure water was then layered on the top of the lower aqueous phase using the microsyringe setup described earlier. This volume was also noted and the absorbance was monitored at regular intervals. When sufficient data were obtained the cuvette was shaken to mix the two solutions and the final absorbance A_∞ was noted. The volume of the lower phase and the measured cross-sectional area gave the value of l_1. It was found to be more accurate to calculate l_2 using the initial and final concentration/absorbance data. The two values of l_2 were later compared to see if they agree satisfactorily. The absorbance data were fitted to the theoretical values (eq 4 was found to be more useful than eq 3) to obtain the diffusivities.

To check if the layering was taking place without significant disturbances, $KMnO_4$ solution was used as the lower fluid. Visual observations showed that sharp interfaces were obtained, but little shocks could give rise to immediate mixing. Further, the accuracy of the method as a whole was checked using KNO_3 for which the diffusivities are known to better than 0.1% accuracy.

There were also some problems with natural convection. In the spectrophotometer used during the earlier trials, the cell was heated from one side. This gave rise to natural convection which was clearly observable when $KMnO_4$ was added. In the spectrophotometer with the reconstructed cell the heater was at the bottom and no natural convection was observed at 30 °C unless the lower liquid was less dense initially. Thus, KNO_3 and SDS solutions were free of such effects. Others (mainly organics) were handled by adding small quantities of KCl to the lower solution making it more dense. Since KCl is transparent in the UV range, the absorbances were not disturbed. Experiments were performed with three different KCl concentrations ($\sim$1 g mL^{-1}). An attempt to extrapolate the results to zero KCl concentration was made, but no changes nor trends were seen and the average values have been reported here.

We simplified some of the restrictions posed by spectrophotometry as well. Spectrophotometry requires that the species under consideration have strong absorption peaks. This rules out many chemicals leaving ones such as aromatics, proteins, etc.; SDS in water has a small peak at about 300 nm. But below the critical micellization concentration (cmc) the peak is almost indistinguishable. We chose 225 nm and required that in such cases we check closely to verify that Beer's law held there. Beer's law was found to be valid for SDS at 225 nm.

In the second set of experiments, a micellar SDS solution of fixed concentration (same solution for all runs), with nitrobenzene as a solubilizate was used as the lower liquid, and squalane was used as the upper liquid. A Hewlett-Packard 8452A diode array spectrophotometer was used. High purity SDS (with the same electrical conductivity as "pure" SDS) was used as purchased from Calbiochem (La Jolla, California). Squalane (Aldrich) was 99% pure and spectroscopically transparent. SDS has a cmc of around 8.2 mM, and SDS solutions were fixed at 30 mM. The SDS solution was contacted with squalane for over 27 h, and the absorbances (190 nm to 400 nm) were swept hourly. Significant changes were seen in the UV range at the very end of the spectrum (190 nm) after large times. These changes were probably due to the presence of unsaturated squalene which formed water-soluble peroxides and were leached into the aqueous phase. It was determined that the amounts of squalene could not have been significant, and such activity stayed well away from 270 nm which was used to monitor nitrobenzene. It was also inferred that SDS was insoluble in squalane and squalane insoluble in SDS solution.

The solubilizate used was nitrobenzene which has a strong absorption peak at 270 nm and hence this was the wavelength chosen. The lower liquid was a SDS solution with nitrobenzene concentrations at 0.027, 0.048, and 0.097 mM in the three runs. The aggregation number for SDS micelles suggested by the supplier is 62. The concentration of micelles was calculated using this number and the concentration of nitrobenzene was kept below the limit of 1 nitrobenzene molecule per micelle. Beer's law holds for nitrobenzene in water and in SDS solution. The key feature here, and the one significant difference with the experiments discussed in the literature, is that there is no net flux of surfactant, only nitrobenzene moves upward into the top (oil) phase. Much higher viscosity of squalane compared to water and an interfacial tension at the aqueous solution−squalane interface as compared to none at the aqueous solution−water interface in the first set of experiments, made the second set of experiments much easier to conduct because of much higher damping effect during layering. After layering, the absorbances were measured for 20−30 h. In no case could we approach conditions sufficiently close to equilibrium nor could we shake the sample after the experiments to hasten equilibrium (as done for the aqueous solution−water system) because of emulsification.

At the end of these runs one special case (case 4 in Table 1) was also tested where the SDS concentration was 60 mM and that of nitrobenzene was 0.097 mM. That is, the SDS concentration was increased while that of nitrobenzene was kept within

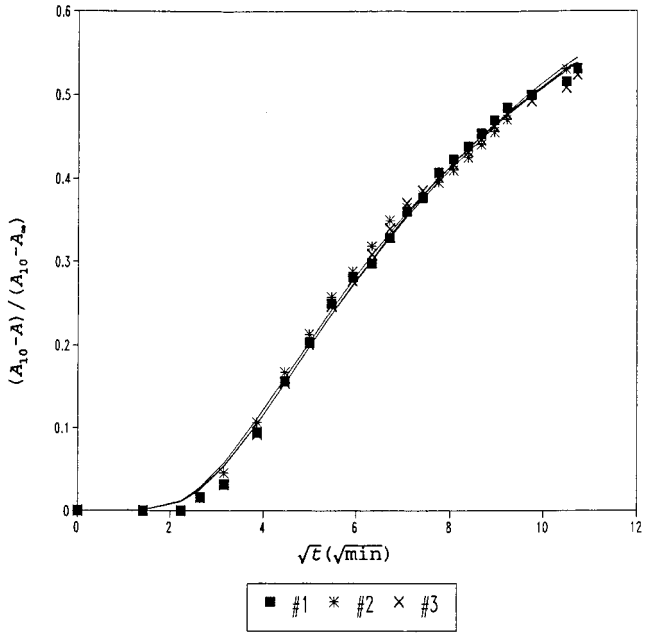

Figure 3. The dimensionless absorbances for KNO_3 are plotted against the square root of time for three cases only. The values of l_2 only are different. The bold lines are from eq 4.

the earlier values. Although the concentrations are quite diffrent, the ratio of concentrations of SDS to nitrobenzene in case 4 is same as that in case 2 in Table 1. Again l_1 was calculated by accurately measuring the layered volume using a micropipet and then dividing with the cross-sectional area. Although the volume of squalane added was known, l_2 was calculated using material balances described later. The two values of l_2 were later compared to check the reliability of the entire process.

Other solutes, such as phenol, *m*-nitrophenol, acidic *p*-nitrobenzoic acid, and β-naphthol, were also tested but failed, with interesting implications to drug delivery discussed in the very last paragraph in the next section.

Results and Discussion

(a) Aqueous Solution + Water Systems. Six experiments were conducted with 1 wt % of KNO_3. KNO_3 has a clear spectrum with a peak at 300 nm which was used to monitor concentrations. The absorbances as a function of time measured in the contacting experiments are shown for three cases in Figure 3. The bold lines are the fitted curves from eq 4. Both l_1 and l_2 were varied. The calculated diffusivities range from (1.833−1.95) $\times 10^{-9}$ m^2 s^{-1}. The average value is 1.862 $\times 10^{-9}$ m^2 s^{-1} compared to 1.846 $\times 10^{-9}$ m^2 s^{-1} for 0.01N solution at 25 °C (CRC Handbook, 1979/80), and the individual values are within 5% of the value reported in the literature.

Aniline, phenol, and nitrobenzene have absorption peaks at around 280 nm. They all require the presence of KCl for stabilization as described previously. Typical results for phenol at 1.55, 0.775, and 0.55 g mL^{-1} of KCl concentrations are diffusivities of 1.27, 1.243, and 1.4 $\times 10^{-9}$ m^2 s^{-1}, respectively. With each experiment done thrice, a total of nine runs, all diffusivities fall within 6% of the average. The other such averages are 1.35 $\times 10^{-9}$ m^2 s^{-1} for aniline, 1.297 $\times 10^{-9}$ m^2 s^{-1} for phenol and 1.411 $\times 10^{-9}$ m^2 s^{-1} for nitrobenzene. We were unable to find published data to compare these to. Nevertheless, the diffusivities appear to be in the expected range.

The UV spectrum for SDS is shown in Figure 4. It has a peak at about 300 nm. However, for the reasons stated earlier

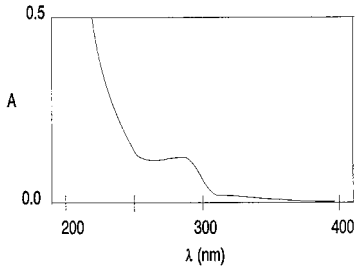

Figure 4. The UV absorption spectrum of SDS.

225 nm was used below the cmc (which at those concentrations lie at the foot of the shoulder). Beer's law does hold here. The results for three different runs (7.5, 5.9, and 5.9 mM) all below cmc of 8.1 mL^{-1}, were used to calculate the diffusivity. The individual data showed no concentration dependence, and their average value was found to be 8.9 $\times 10^{-10}$ m^2 s^{-1}. Using the values of tracer self-diffusion coefficients of the sodium ion, 1.35 $\times 10^{-9}$ cm^2 s^{-1},[6] and that of the dodecyl sulfate ion, 5.7 $\times 10^{-10}$ cm^2 s^{-1},[15] one can calculate the effective diffusivity D_e of SDS using Nernst rule:

$$\frac{2}{D_e} = \frac{1}{D_{Na^+}} + \frac{1}{D_{DS^-}} \tag{9}$$

The calculated value is 8.02 $\times 10^{-10}$ cm^2 s^{-1}, with about 9% deviation. The values for the NMR self-diffusion coefficients of sodium and dodecyl sulfate ions[20] are very close to those listed earlier, but there is some scatter in this low concentration range. It is being assumed here that at concentrations below cmc the system can be characterized as "infinitely dilute," where the mutual diffusion coefficient measured should be equal to the self-diffusion coefficient.

The diffusivity of SDS was also measured at a concentration above cmc (68 mM). The advantage of using this system is it has a strong absorption peak at 300 nm. The diffusivity of 6.8 $\times 10^{-9}$ m^2 s^{-1} obtained from there is only an effective value since the diffusivities are concentration dependent. The value is almost twice the value at 68 mM obtained by Weinheimer et al.[36] The implications from the standpoint of demicellization have been discussed elsewhere by Neogi.[26]

These results confirm that the present experimental setup provides good results even under adverse conditions including poor adsorption and the lack of damping during layering. Whereas the aqueous solution−water experiments are difficult to perform, the results are easy to interpret. The opposite is true in the aqueous solution-squalane system discussed next.

(b) Aqueous Solution + Squalane Systems. Following Liapis et al.[17] and Heeter and Liapis[12] the experimental data were fitted to

$$\langle c_1 \rangle = x_1 + x_2 \exp(-x_3 t) + (c_{1o} - x_1 - x_2)\exp(-x_4 t) \tag{10}$$

where the x's are parameters, of which x_1 is the equilibrium concentration. The final parameters to be obtained are D_1, D_2, k_i, and K. Although l_2 is known, it is more accurate to calculate it through the material balance

$$(l_2 - l_1)\, x_1/K + l_1 x_1 = l_1 c_{1o} \tag{11}$$

Later, the two values of l_2 can be compared to check the overall accuracy. The total number of parameters in eq 10 and eq 8 are the same. It was noted earlier that the inversion of eq 8 would result in an infinite sum of exponentials. However, the param-

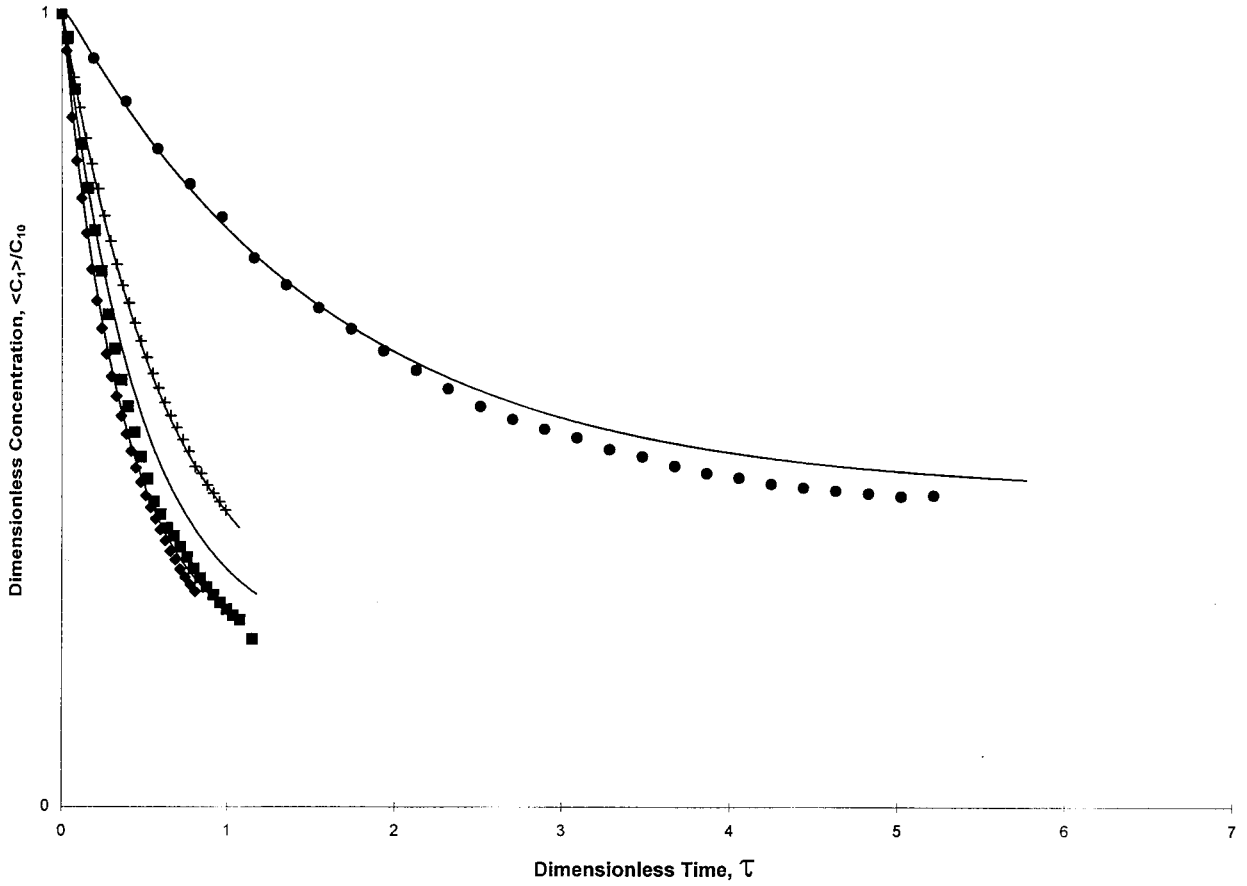

Figure 5. Comparison between the experimental data and theory. The largest deviation is less than 9%. The plots are from the bottom to top 1, 2, 4, and 3 as detailed in Table 1. The comparison improves in appearance, but not numerically, if the dimensionless time is tD_1/l_1^2 instead of $tD_2/(l_2 - l_1)^2$ used here.

eters in a series are not independent of one another, except for the first four. As a result, if the number of terms in eq 10 is increased and fitted to the experimental data, then many sets of solutions are found with exactly the same residual sum of squares.

Fitting eq 10 to the data was found to be very difficult and eventually an optimizer program called MINOS 5.4[25] was used. The Laplace transform of eq 10

$$\overline{\langle c_1 \rangle} = \frac{x_1}{s} + \frac{x_2}{s + x_2} + \frac{(c_{1o} - x_1 - x_2)}{s + x_4} \qquad (12)$$

was fitted to eq 8 at selected real values of s over a range of s, the upper and lower limits of which have been determined following the rules given by Liapis et al.[17] and Heeter and Liapis.[12] This gave us the values of the unknowns D_1, D_2, k_i, and K. The values of these parameters are shown in Table 1, and the fit is also shown in Figure 5. The program (MINOS) reports the parameter values, residual sum of squares, and a dimensionless measure of the gradient using the Jacobian, at every iteration, and "converges" when this gradient is less 10^{-10}. Subsequently, the program was run again using all these values as initial guesses except for one, which was perturbed by 50%, and the program most often returned the old values in one or two iterations attesting to the soundeness of the convergence criterion. If all values were perturbed, the program usually converged to a new value. Sets of these results were studied, and among those where the parameter values were physically realsitic, the one with the lowest residual sum of squares was chosen. Once the process was completed, the final parameter values were used to solve eqs 5−7 numerically using finite difference with forward time and central space. These are the curves shown in Figure 5. The largest error in fitting is less than 9%. The interfacial resistances are very high as are the resistances to diffusion in squalane. Hence Figure 5 has been drawn with dimensionless time $\tau = tD_2/(l_2 - l_1)^2$ to emphasize the significant resistance in the oil phase. The data cover a wide range, but always stay away from equilibrium which is probably why the fitted curves tend to overpredict the equilibrium concentrations.

The fact that interfacial resistances are high can be checked by looking at some form of Damköhler number using k_i as a reaction rate against diffusion rates, providing low values (irrespective of which diffusivity or length scale is used) instead of a classical value of infinity. The averages and the maximum deviations from the averages shown indicate that k_i is also the only quantity that is significantly changed on increasing the surfactant concentration. The interfacial resistance increases as the surfactant concentration is increased. Investigation of a related problem, of dynamics of adsorption of a surfactant at a micellar solution-air interface, has shown that adsorption−desorption rates were quantitatively linked to the micellization−demicellization kinetics.[35] This is understandable. Micelles have to first demicellize before the surfactant molecules can be adsorbed. Similarly, micelles have to demicellize before they can yield the solubilizate to the oil phase at the oil−water interface. It is seen here that the interfacial resistance increases with increasing surfactant concentration (k_i decreases by a factor of 20), which implies that the characteristic time for micellization-demicellization should increase with surfactant concen-

tration. Indeed it does so for micelles without solubilizate[14] and by about a factor of 10 in that concentration range, but no data appear to exist where the effects of solubilizates have been included as suited to the present application. The reverse problem of solubilization has been correlated to micellization-demicellization as well.[28]

It is puzzling as to why the diffusivity of nitrobenzene in the micellar solution is so high. Originally we were expecting this diffusivity to be low and near that of a micelle. However, the NMR self-diffusivities of the solubilizates are unexpectedly high, according to one review.[20]

Some runs with nitrobenzene only in water, that is, no surfactant, were also conducted. Investigation of the data showed that the projected nitrobenzene concentrations in water at equilibrium were very low, in fact lower than the limit of our observations. This implies that K and c_1 at the interface, are approximately zeroes. In the model, this leads to decoupling of the transport in the two phases, and hence, to the conclusion that the data from the lower phase cannot be used reliably to estimate the parameters governing the dynamics in the upper phase.

Phenol, *m*-nitrophenol, and acidic *p*-nitrobenzoic acid are all insoluble in squalane from both aqueous solution and the micellar solution, that is, they will not partition into squalane. But β-naphthol is soluble in squalane when contacted with an aqueous solution but insoluble when contacted with a micellar solution with β-naphthol as a solubilizate. That is, β-naphthol prefers micelles to squalane. A drug of this kind cannot be delivered with a micellar solution. It is obvious that some of these partition coefficients need to be measured carefully to understand the efficacy of drug delivery. At present time, this is done empirically using the Meyer−Overton rule, according to which the effectiveness increases as the partition coefficient in water-*n*-octanol falls,[33] where the partition coefficient is defined as the concentration in water/concentration in *n*-octanol. We were able to calculate this partition coefficient to be about 0.064 for nitrobenzene, compared to an average value of 0.0851 for micellar solution/squalane system. The partition coefficient of nitrobenzene in a water/squalane system was estimated to be in a very low range, 0.009, and its water/micelle partition coefficient was about 0.1. The others could not be measured using a spectrophotometer. A more complete view will need both an extensive investigation and measurements with much higher accuracies.

In summary, we note that we have provided for the first time a system which can be analyzed to the extent that the interfacial resistance can be factored out. Most experimental setups, for instance the one used by Carroll,[3] can only be partially analyzed, and succeeds only because the interfacial resistance is in control. We have shown the reliability of our experimental setup in simple systems and proceeded to analyze more complex ones, which are the systems containing surfactants where interfacial resistance can be important. The results show that they are indeed significant. The most important contribution here is that we have provided a mathematical model for the interfacial resistance and obtained the parameter values that shed further light into the nature of the interfacial resistance, in that they are probably related to the kinetics of surfactant structure formation/breakdown. In addition, we can use the present model to explain why Chen et al.[5] obtain constant rates of solubilization in their experiments. The interfacial flux from eq 7 is k_i (concentration of pure oil − K times concentration of the oil in the micellar solution). Now the concentration of the pure oil (c_o) is a constant, and at least at short times, the concentration of oil in the micellar solution is negligible. This leads to constant flux at the interface if the interfacial resistance is controlling. In case of Chen et al.[5] the conservation of oil in the drop leads to

$$-\frac{\mathrm{d}}{\mathrm{d}t}\left(c_o\frac{4}{3}\pi R^3\right) = k_i c_o 4\pi R^2$$

where R is the drop radius, and eventually to $\mathrm{d}R/\mathrm{d}t$ = constant. Carroll[3] actually reports the constant values of k_i times a fixed experimental parameter. This offers the evidence the model obtained is of general validity, and not confined to the specific case studied here.

Acknowledgment. The authors thank Professors Sitton and Forciniti for the use of their laboratories and expertise, Professor Sourlas for the use of the optimization programs, and Professor Liapis for consultations on parameter estimation in Laplace domain, and, finally but not the least, Scott Moll for his help with the plots.

References and Notes

(1) Anandakrishnan, K.; Neogi, P.; Friberg, S. E. Mass transfer analysis in a surfactant system. *Colloid Surfaces* **1992**, *64*, 197.

(2) Armstrong, D. W.; Ward, T. J.; Berthod, A. Micellar effects on molecular diffusion: theoretical and chromatographic considerations. *Analytical Biochem.* **1986**, *58*, 579.

(3) Carroll, B. J. The kinetics of solubilization of nonpolar oils by nonionic surfactant solution. *J. Colloid Interface Sci.* **1981**, *79*, 126.

(4) Chan, A. F.; Evans, D. F.; Cussler, E. L. Explaining solubilization kinetics. *AIChE J.* **1976**, *22*, 1006.

(5) Chen, B.-H.; Miller, C. A.; Garrett, P. R. 1997 Rates of solubilization of triolein into nonionic surfactant solutions. *Colloids Surfaces A 128*, 129.

(6) Clifford, J.; Pethica, B. A. Properties of a micellar solution. *Trans. Faraday Soc*. **1964**, *60*, 216.

(7) *CRC Handbook of Physics and Chemistry*, 60th ed.; CRC Press: Boca Raton, 1979/1980.

(8) Friberg, S. E.; Ma, Z.; Neogi, P. Temporary liquid crystals in microemulsions systems. In *Surfactant Based Mobility Control*; Smith, D. H., ed.; American Chemical Society: Washington, DC, 1989; p 108.

(9) Friberg, S. E.; Mortensen, M.; Neogi, P. Hydrocarbon extraction into surfactant phase with nonionic surfactants. I. Influence of phase equilibria for extraction kinetics. *Sep. Sci. Technol.* **1985**, *20*, 285.

(10) Grimberg, S. J.; Aitken, M. D.; Stringfellow, W. T. The influence of a surfactant on the rate of phenanthrene mass transfer into water. *Water Sci. Technol.* **1994**, *30*, 23.

(11) Hadkar, U. B.; Angane, V. M. Critical Concentration of surfactants through diffusion studies. *Indian Drugs* **1995**, *32*, 236.

(12) Heeter, G. A.; Liapis, A. I. Affinity adsorption of adsorbates into spherical monodisperse and bidisperse porous perfusive and purely diffusive adsorbent particles packed in a column. Parameter estimation in the Laplace transform domain. *J. Chromatography* **1997**, *760*, 55.

(13) Kabalnov, A. S. Can micelles mediate a mass transfer between oil droplets? *Langmuir* **1994**, *10*, 680.

(14) Kahlweit, M. Kinetics of formation of association colloids. *J. Colloid Interface Sci.* **1982**, *90*, 92.

(15) Kamenka, N.; Lindman, B.; Brun, B. Translational motion and association in aqueous sodium dodecyl sulphate solutions. *Trans. Faraday Soc.* **1974**, *252*, 144.

(16) Lawrence, M. J. Surfactant System: Their use in drug delivery. *Chem. Soc. Rev.* **1994**, *23*, 417.

(17) Liapis, A. I.; Tongta, A.; Crosser, O. C. Finite bath affinity adsorption of absorbates into spherical porous adsorbent particles: Parameter estimation in the Laplace domain. *Math. Modelling Sci. Computing* **1995**, *5*, 1.

(18) Lim, J. C.; Miller, C. A. Predicting Conditions for Intermediate phase formation in surfactant systems. *Prog. Colloid Polym. Sci.* **1990**, *83*, 29.

(19) Lim., J. C.; Miller, C. A. Dynamic behavior and detergency in systems containing nonionic surfactants and mixtures of polar and nonpolar oils. *Langmuir* **1991**, *7*, 2021.

(20) Lindman, B.; Kamenka, N.; Puyal, M. C.; Rymdén, R.; Stilbs, P. Micelle formation in anionic and cationic surfactants from fourier transform hydrogen-1 and lithium-7 nuclear magnetic resonance and tracer self-diffusion studies. *J. Phys. Chem.* **1984**, *88*, 5048.

(21) Lindman, B.; Stilbs, P. Molecular diffusion in microemulsions. In *Microemulsions: Structure and Dynamics*; Friberg, S. E., Bothorel, P., Eds.; CRC Press: Boca Raton, 1987; p 119.

(22) Ma, Z.; Friberg, S. E.; Neogi, P. Observation of temporary liquid crystals in water-in-oil microemulsion systems. *Colloid Surfaces* **1988**, *33*, 249.

(23) Ma, Z.; Friberg, S. E.; Neogi, P. Single component mass transfer in a cosurfactant−water-surfactant system. *AIChE J.* **1989**, *35*, 1678.

(24) Muramatsu, N.; Minton, A. P. An automated method for rapid determination of diffusion coefficients via measurements of boundary spreading. *Anal. Biochem.* **1988**, *168*, 345.

(25) Murtagh, B. A.; Saunders, M. A. 1995 *MINOS 5.4 User's Guide*; Stanford University: Palo Alto, CA.

(26) Neogi, P. Diffusion in a micellar solution. *Langmuir* **1994**, *10*, 1410.

(27) Neogi, P.; Kim, M.; Friberg, S. E. Hydrocarbon extraction into surfactant phase with nonionic surfactants. II. Model. *Sep. Sci. Technol.* **1985**, *20*, 613.

(28) Oh, S. G.; Shah, D. O. The effect of micellar lifetime on the rate of solubilization and detergency in sodium dodecyl sulfate solutions. *J. Am. Chemists' Soc.* **1993**, *70*, 673.

(29) Raney, K.; Benton, W. J.; Miller, C. A. 1985 Use of videomicroscopy in diffusion studies of oil−water-surfactant system. In *Macro- and Microemulsions*; Shah, D. O., ed.; ACS Symposium Series; Washington, DC, 1985; p 193.

(30) Raney, K. H.; Miller, C. A. Diffusion path analysis of dynamic behavior of oil−water-surfactant systems. *AIChE J* **1987**, *33*, 1791.

(31) Rang, M. J.; Miller, C. A. Spontaneous emulsification of oil drops containing surfactants and medium chain alcohol. *Prog. Colloid Polym. Sci.* **1998**, *109*, 101.

(32) Rang, M. J.; Miller, C. A.; Thunig, C.; Hoffman, H. H. Dynamic behavior of alcohol drops in dilute solutions of an amine oxide surfactant. *J. Colloid Interface Sci.* **1995**, *175*, 440.

(33) Seeman, P. The membrane actions of anesthetics and tranquilizers. *Pharmacol. Rev.* **1972**, *24*, 583.

(34) Shaeiwitz, J. A.; Chan, A. F.-C.; Cussler, E. L.; Evans, D. F. The mechanisms of solubilization in detergent solutions. *J. Colloid Interface Sci.* **1981**, *84*, 47.

(35) Vlahovsky, P. M.; Horozov, T.; Dushkin, C. D.; Kralchevsky, P. A.; Mehreteab, A.; Bronze, G. Adsorption from micellar surfactant solutions: Nonlinear theory and experiments. *J. Colloid Interface Sci.* **1997**, *183*, 223.

(36) Weinheimer, R. M., Evans, D. F., and Cussler, E. L. Diffusion in surfactant solution. *J. Colloid Interface Sci.* **1981**, *80*, 357.